
A Latent-Variable Grid Model

Rajasekaran Masatran

MASATRAN@FREESHELL.ORG

Computer Science and Engineering, Indian Institute of Technology Madras

Abstract

A major problem with the conditional random field (CRF) is that its learning algorithms are computationally expensive. Grid associative CRFs occur frequently in sequence and image learning. We design a non-markov high-bias low-variance model as an alternative to this subclass of CRF. Our learning algorithm uses vector quantization and, at time complexity $O(T^d \log T^d)$, is significantly faster than that of CRF.

1. Introduction

Grids of random variables occur in many fields. The one-dimensional case (sequences and time series) occurs in natural language processing, computational biology and speech recognition. The two-dimensional case occurs in images. The three-dimensional case occurs in videos. Statistical modeling of these networks enables segmentation, classification and clustering. The conditional random field (CRF) is one popular approach to modeling networks, including grids. A major problem with CRF is that its learning algorithms are computationally expensive. Besides, many of them do not have tight computational complexity bounds. However, there are commonly occurring subsets of the set of CRFs for which fast algorithms with tight computational complexity bounds are feasible. One such subset is the set of grid associative CRFs. Ours is a model-centric approach, and is similar to the (Prince, 2012) approach to computer vision.

1.1. Latent-Variable Models

We consider a subset of the set of latent-variable models. The output symbols, which are the visible variables, are modeled on a set of corresponding nodes, which are the latent variables. The value of each visible variable is dependent on its latent variable. Given the values of all latent variables, the visible variables are independent of each other. A latent-variable model where all dependencies are undirected is an CRF.

1.2. Grid

Instead of considering general networks, we restrict our domain to d -dimensional grids. There are T nodes along each dimension. Each node t is an element of $\{1 \cdots T\}^d$. We denote the grid by T^d . Without loss of generality, we assume that the grid has the same length in all dimensions. The real-vector variant that we will discuss in section 4 is essentially a vector field.

1.3. Associativity

In a latent-variable model, if adjacent latent nodes share the same set of possible states, and are likely to be in the same state, this is called associativity. This is an intrinsic property of the process underlying many application domains. The amount of associativity in the grid varies by domain. For instance, in the one-dimensional case, there is a lot of associativity in speech recognition, a limited amount of associativity in chunking of natural language, and almost no associativity in part-of-speech tagging in natural language.

1.4. Inertia

Associativity is restricted to dependency between adjacent latent nodes. In this paper, we consider a broader condition, where non-adjacent latent nodes are dependent on each other. This is not markov, but is related to an n^{th} -order markov model. We call this inertia, and restrict our model to grids with inertia. Since an inertial model can approximate an associative model, it can be used for: (1) Applications with inertia in the grid, as well as (2) Approximation of applications with associativity in the grid.

1.5. Using Stochastic Models

An assignment of observed symbol to each visible variable is an image. The image is essentially the visible-variable grid, as opposed to the latent-variable grid. Our training data consists of images, and lacks the state configuration of the corresponding latent variables.

In classification of images, the input is a set of classes that are specified by a set of images belonging to each. The objective is to classify test images into these classes. We build

a model for each class by learning a class-conditional density for its grid configurations. Given the prior probabilities and these class-conditional models, bayesian classification is used to classify test images.

Among latent-variable models, the CRF is popular for constructing the class-conditional density. The hidden markov model (HMM) is popular for the one-dimensional case. The model we design in this paper is an inertial non-markov alternative to associative CRF and HMM, for constructing the class-conditional density.

1.6. Contributions

1. A latent-variable statistical model for grid-structured data: a variant each, for the discrete case (Section 4) and the real case (Section 5)
2. An index for associativity (Subsection 3.1): a variant each, for the directed case and the undirected case
3. An index for inertia (Subsection 3.2)

1.7. Outline

In *Section 1: Introduction*, we motivate the problem; describe latent-variable models, the grid, associativity and inertia; explain how stochastic models are used; summarize contributions; and give an outline.

In *Section 2: Background*, we review prior work, discuss mathematical background: markov chain and HMM, and give intuition about our model.

In *Section 3: Associativity and Inertia*, we propose indices for associativity and inertia, and explain associativity in HMM and CRF.

In *Section 4: Our Model*, we describe our model. We describe sliding window in 3.1, bias-variance tradeoff in 3.2, signature in 3.3, and dependencies between algorithms in 3.4. We describe the six algorithms: evaluation in 3.5, markov correction in 3.6, decoding in 3.7, assign in 3.8, learning in 3.9, and vector quantization in 3.10. We tabulate our time complexities in 3.11.

In *Section 5: Extension to Real Symbols*, we extend our model to real symbols, using a similar structure as section 3.

In *Section 6: Conclusion*, we summarize our contributions, list advantages and disadvantages, and suggest directions for future work.

2. Background

Directed graphical models for sequences were the first graphical models to be studied. (Baum & Petrie, 1966) introduced HMM. (Jelinek, 1969) pioneered their use in

speech recognition. (Baker, 1975) commercialized their use in the Dragon system. (Beal et al., 2002) modified HMM into a model with continuous state, using dirichlet processes. (Montañez et al., 2015) developed an inertial HMM.

Graphical models for general networks were introduced in (Pearl, 1988). (Blake et al., 2011) discussed MRF applications in computer vision. (Wallach, 2002) is an introduction to CRF.

In *Physics*, the Ising model is widely used. The Potts model, described in (Wu, 1982), is a generalization of the Ising model, and is closely related to CRF.

Our algorithm can be formulated as a *kernel method*. The string kernel of (Leslie et al., 2002) is a kernel method that is effective in biological sequence learning.

Our main benchmark is the fast learning algorithm for associative MRF in (Taskar et al., 2004). We solve a slightly different problem, and our solution should be useful in approximating a solution to associative CRF as well. Another potential benchmark is the algorithm for fast inference in associative pairwise MRF in (Boykov et al., 2001).

2.1. Markov Chain

$S = \{S_1, S_2, \dots, S_j, \dots, S_N\}$ is the set of states. The system is in one of these states, and the state is visible. At discrete times, the system undergoes a change of state, according to a set of probabilities associated with the state. The time instants of state changes are $t = \{1, 2, \dots, T\}$, and the state at time t is q_t . $Q = \{q_1, q_2, \dots, q_T\}$.

For a markov system, $P(q_t | q_{t-1}, q_{t-2}, \dots) = P(q_t | q_{t-1})$. Since $P(q_t | q_{t-1})$ is independent of time, we have the set of state transition probabilities $a(i, j) = P(q_t = S_j | q_{t-1} = S_i)$. $\pi(j) = P(q_1 = S_j)$ denotes the initial state probabilities. The parameter set of the markov chain is $\langle A, \pi \rangle$.

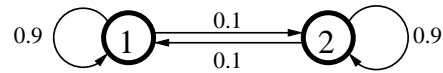


Figure 1. Markov Chain

Figure 1 is a markov chain, with parameters: $S: \{1, 2\}$, $A: \begin{pmatrix} 0.9 & 0.1 \\ 0.1 & 0.9 \end{pmatrix}$.

2.2. Hidden Markov Model

HMM is the commonly-used latent-variable model for sequences. It is based on the markov chain. It is formulated in terms of three problems in (Rabiner, 1989). Unlike in the markov chain, the hidden markov model has a latent state. Each instance of the state emits an observation, and the probability distribution of the observation depends solely on the state from which it is emitted. The model is

a doubly embedded stochastic process: an underlying latent stochastic process that is observed through another set of stochastic processes that produce the observations. The observation sequence is $O = \{o_1, o_2, \dots, o_T\}$. The parameter set of HMM is $\lambda = \langle A, B, \pi \rangle$:

$N = |S|$; $S = \{S_1, S_2, \dots, S_j, \dots, S_N\}$ are the unique states in the model, and the state at time t is q_t .

$M = |V|$; $V = \{v_1, v_2, \dots, v_k, \dots, v_M\}$ are the unique observation symbols, and the symbol at time t is o_t .

$A = \{a(i, j)\}$; $a(i, j) = P(q_t = S_j | q_{t-1} = S_i)$, the state transition probability distribution.

$B = \{b(j, k)\}$; $b(j, k) = P(o_t = v_k | q_t = S_j)$, the observation symbol probability distribution in state j .

$\pi = \{\pi(j)\}$; $\pi(j) = P(q_1 = S_j)$, the initial state probability distribution.

2.3. Intuition

$\{(p_1, p_2, \dots, p_n) \in \mathbb{R}^M \mid \sum_{k=1}^n p_k = 1, p_k \geq 0\}$ is the standard $(M - 1)$ simplex, and is the range of the probability mass for a multinomial distribution with M categories. The states of a HMM can be considered points in the probability simplex. The coordinates of the state are the observation symbol probability distribution B . These coordinates, along with the transition probability distribution A , and the initial state distribution π , together characterize the HMM.

The markov chain can be considered a special case of HMM, where the set of states is precisely the set of corners of the probability simplex. Each state is associated with a single symbol that it emits with probability 1.

3. Associativity and Inertia

We discuss inertia to motivate and understand our model. We also discuss associativity, as it is a simpler alternative to inertia for markov models.

3.1. An Index for Associativity

We propose an index for associativity: $\log_N(\text{tr}(A))$ for the directed case, and $\log_N(N \text{tr}(A))$ for the undirected case. It is 0 when adjacent nodes are uncorrelated, and 1 when adjacent nodes are always in the same state. It is negative infinity when adjacent nodes are never in the same state. Our model should be applicable when this index is atleast, say, 0.5, i.e., $\text{tr}(A) \geq \sqrt{N}$.

3.2. An Index for Inertia

We use a sliding hypercube window to define an index for inertia: $\mathbb{E} \left[\sqrt{\sum_j p_j^2} \right]$. The expectation is taken over the

hypercube centered at the node, for every node in the grid. p_j is the probability of state S_j in the window. It is 1 when all nodes in the window are in the same state, and $\frac{1}{\sqrt{N}}$ when all states have equal probability within the window. Our model should be applicable when this index is atleast, say, 0.9.

3.3. Associativity in HMM

In the following figures, each circle is a HMM/CRF node. The thick circles are latent-variable nodes. The directed edges are transition probabilities and the undirected edges are emission probabilities. Differences between the following HMMs are highlighted in bold.

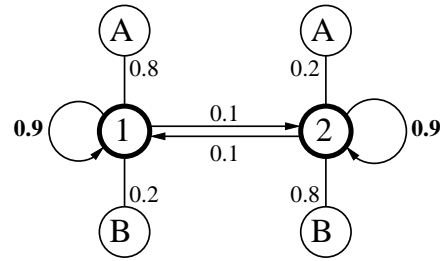


Figure 2. Associative HMM

Figure 2 is a HMM that avoids changing state. It has parameters: $S: \{1, 2\}$, $V: \{A, B\}$, $A: \begin{pmatrix} 0.9 & 0.1 \\ 0.1 & 0.9 \end{pmatrix}$, $B: \begin{pmatrix} 0.8 & 0.2 \\ 0.2 & 0.8 \end{pmatrix}$. The index of associativity is: $\log_2(\text{tr}(\begin{pmatrix} 0.9 & 0.1 \\ 0.1 & 0.9 \end{pmatrix})) = \log_2(0.9 + 0.9) = +0.848$.

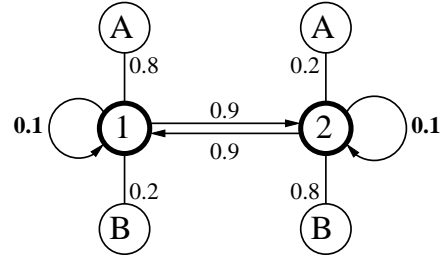


Figure 3. Non-Associative HMM

Figure 3 is a HMM that changes state frequently. It has parameters: $S: \{1, 2\}$, $V: \{A, B\}$, $A: \begin{pmatrix} 0.1 & 0.9 \\ 0.9 & 0.1 \end{pmatrix}$, $B: \begin{pmatrix} 0.8 & 0.2 \\ 0.2 & 0.8 \end{pmatrix}$. The index of associativity is: $\log_2(\text{tr}(\begin{pmatrix} 0.1 & 0.9 \\ 0.9 & 0.1 \end{pmatrix})) = \log_2(0.1 + 0.1) = -2.322$.

3.4. Associativity in CRF

Figure 4 is an associative CRF, while Figure 5 is a non-associative CRF. The matrices are pairwise potentials, and the main diagonal represents adjacent nodes being in the same state. All nodes, latent and visible, are boolean. Differences between the following CRFs are highlighted in bold.

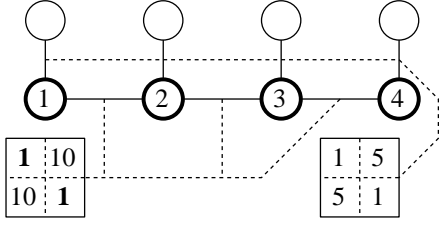


Figure 4. Associative CRF

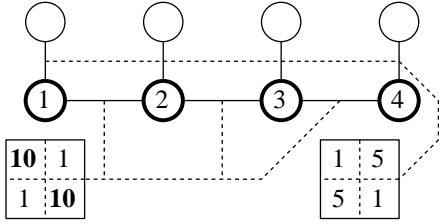


Figure 5. Non-Associative CRF

4. Our Model

In this section, we describe the variant of our model for discrete output symbols. The one-dimensional case of this variant can be used to model, for instance, proteins, which are sequences of twenty amino acids.

The signature, discussed in section 3.3, maps the node into the probability simplex. We divide the probability simplex into partitions, and a partition corresponds to a state in HMM. The probability of transitioning between partitions is A , and the observation symbol probability distribution is B . Roughly, this is our data model, and our algorithms conform to it, but not completely. Our model is not markov. It has inertia. The parameter set of our model is $\phi = \langle A, B, w \rangle$, the same as that of HMM, with π removed, and w , the size of the sliding window, added.

4.1. Sliding Window

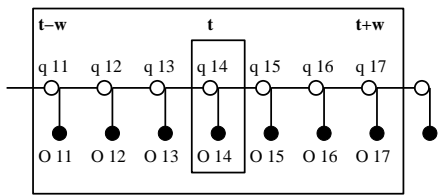


Figure 6. Sliding Window

Sliding window methods are popular for sequences (Dietterich, 2002) and images. Since our model has inertia, nearby nodes are probably in the same state. Therefore, sliding window models are likely to work well. At t , the w -window is the hypercube from $(t - \lceil w, w, \dots \rceil)$ to $(t + \lceil w, w, \dots \rceil)$. It might be beneficial to use different values of w for evaluation, decoding and learning: w_e for evaluation, w for decoding, and w_l for learning.

$R(t)$ is the set of $2d$ nodes adjacent to node t .

4.2. Bias-Variance Tradeoff

The optimal size of the window is related to the typical minimum number of steps in the same direction before a change of state. Increasing the window size increases inductive bias, and reduces variance. Reducing the window size reduces inductive bias, and increases variance.

4.3. Signature

Our decoding algorithm works in two steps: (1) Characterize the sliding window around the current time step with a signature, and (2) Use this signature to assign a latent state to the current time step. The signature X is that observation probability vector with maximum likelihood of generating the symbols in the sliding window. $X = \{x_t(k)\}$ where $x_t(k)$ is the sample probability of symbol v_k in the w -window around time t . This signature is a point in the probability simplex.

4.4. Algorithms and their Dependencies

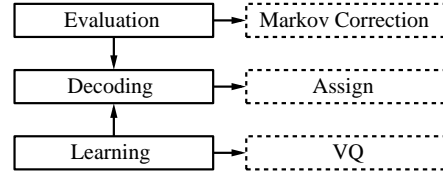


Figure 7. Algorithms and their dependencies

4.5. Evaluation

Given the model $\phi = \langle A, B, w \rangle$ and the image O , compute the probability $P(O|\phi)$ that the image was produced by the model.

Algorithm 1: Evaluation ($O(MNT^d)$)

Input: A, B, w_e, O

Output: p

$(X, Q) \leftarrow \text{decoding}(B, w_e, O)$ $O(MNT^d)$

$p \leftarrow 1$

for $t \in T^d$ **do**

$p \leftarrow p \cdot b(q_t, o_t) \sqrt{\prod_{r \in R(t)} \alpha(X, t) a(q_t, q_r)}$

Represent in log domain to prevent underflow.

end

Algorithm 1: Since we have inertia, the results of the decoding algorithm are reliable, and we do not need to consider all possible grid configurations. We decode the grid configuration from the image, and use that to compute the likelihood.

4.6. Markov Correction

$0 < \alpha(X, t) \leq 1$ corrects for assuming the markov property in the evaluation step though it is not present in this model. Experimental evaluation is required to determine typical values.

4.7. Decoding

Find the grid configuration $Q = \{q_t\}_{t \in T}$, given the model $\phi = \langle A, B, w \rangle$ and the image O .

Algorithm 2: Decoding ($O(MNT^d)$)

Input: B, w, O

Output: X, Q

Initialize $_{v_k \in V} \text{symcount}(v_k)$

```

for  $t \in T^d$  do  $O(MNT^d)$ 
     $x_t \leftarrow \frac{\text{symcount}}{M}$ 
     $q_t \leftarrow \text{assign}(B, x_t)$   $O(MN)$ 
    increment  $\text{symcount}(\text{newwindow} - \text{oldwindow})$ 
    decrement  $\text{symcount}(\text{oldwindow} - \text{newwindow})$ 
end

```

Algorithm 2: To decode the grid, we initialize the sliding window and compute the symbol counts (*symcount*) in it. We slide the sliding window through the grid, and in every step, update the symbol counts, and send the signature of the sliding window to *assign* to get the node state.

4.8. Assign

The *assign* subroutine finds the node state $q_t \in S$, given the model $\phi = \langle A, B, w \rangle$ and the node signature x_t .

Algorithm 3: Assign ($O(MN)$)

Input: B, x_t

Output: q_t

```

for  $j \leftarrow 1$  to  $N$  do  $O(MN)$ 
     $\text{dist}(j) \leftarrow \|x - B(j)\|$ 
end
 $q_t \leftarrow \min \text{index}_j(\text{dist}_j)$ 

```

Algorithm 3: Since the model has inertia, we reduce computational complexity of assigning state by assuming that neighboring nodes probably have the same state as the current node.

The node signature x_t is a probability distribution. The *assign* subroutine assigns t to that state j for which $B(j)$ is the closest to x_t , as per L_2 norm. This creates a partitioning of the probability simplex into partitions, each of which is associated with a state.

4.9. Learning

Optimize the model parameters $\phi = \langle A, B, w \rangle$ to best describe the image, i.e., maximize $P(O|\phi)$.

Algorithm 4: Learning ($O(MT^d \log T^d)$)

Input: O, w_l

Output: A, B

Initialize $_{v_k \in V} \text{symcount}(v_k)$

```

for  $t \in T^d$  do  $O(MT^d)$ 
     $x_t \leftarrow \frac{\text{symcount}}{M}$   $O(M)$ 
    increment  $\text{symcount}(\text{newwindow} - \text{oldwindow})$ 
    decrement  $\text{symcount}(\text{oldwindow} - \text{newwindow})$ 
end
 $(B, Q) \leftarrow VQ(X)$   $O(MT^d \log T^d)$ 
     $B$  is assigned the VQ codebook.
for  $t \in T^d$  do  $O(T^d)$ 
    increment  $\text{statecount}(q_t)$ 
    for  $r \in R(t)$  do
        increment  $A'(q_t, r)$ 
    end
end
for  $j \leftarrow 1$  to  $N$  do
     $A(j) \leftarrow \frac{A'(j)}{2 \text{d statecount}(j)}$ 
end

```

Algorithm 4: Since we have inertia, our decoding algorithm is reasonably reliable. We decode the image, and use the grid configuration to learn the parameters of the model.

We compute the signature at all nodes using symbol counts (*symcount*). Vector quantization on the signatures partitions the probability simplex into states. The coordinates of the centroids are the observation probability matrix, and the sample transition probabilities in the grid of signatures are the state transition probability matrix.

4.10. Vector Quantization

Our requirements for clustering are: (1) Roughly spherical partitions, and (2) A representative point for each partition. We solve our clustering problem as vector quantization (VQ) since the requirements are similar. VQ is a classical problem in data compression, and has multiple algorithms with different tradeoffs. Fast pairwise nearest neighbor (Fast PNN) from (Equitz, 1989) is a VQ algorithm that trades modeling accuracy for reduced computational complexity. We use Fast PNN as it has $O(n \log n)$ computational complexity, and we do not need high modeling accuracy in VQ.

4.11. Time Complexity

	Our Model
Evaluation	$O(MNT^d)$
Decoding	$O(MNT^d)$
Learning	$O(MT^d \log T^d)$

Table 1. Time Complexity

5. Extension to Real Symbols

In the previous section, we modeled grids of discrete symbols. In this section, we describe the variant of our model for real-valued output symbols. The one-dimensional case of this variant is essentially scalar/vector time series. The two-dimensional case of this variant can model digital images, in grayscale pixel value, or in extracted features. This section is self-contained and may be skipped if not required.

Previously, the state variable took values in the probability simplex embedded in \mathbb{R}^M , where M was the number of unique observation symbols. Now, it consists of M real variables representing the mean vector, i.e., it is a M -dimensional vector and has range \mathbb{R}^M . The observation grid is essentially a vector field. $o_t = \{o_{t,1}, o_{t,2}, \dots, o_{t,M}\}$. The parameter set of this variant is $\psi = \langle A, \mu, \Sigma, w \rangle$.

When each point is assigned to the closest state, the state space gets divided into partitions, each of which corresponds to a state in HMM. Matrix A remains the probability of transitioning between partitions, and w remains the size of the sliding window. We modify the other parameters of our model as follows:

$M = |V|$ was the number/set of unique observation symbols. Instead, now the observation symbol o_t is in \mathbb{R}^M .

B was the observation symbol probability distribution. It is replaced by μ and Σ .

$\mu = \mu(j, k)$; where $\mu(j)$ is the sample mean of state S_j .

$\Sigma = \Sigma(j, i, k)$; where $\Sigma(j)$ is the sample covariance matrix of state S_j .

5.1. Prior Work

Real-symbol HMM is discussed in subsection IV-A of (Rabiner, 1989). Switching linear dynamical systems (LDS) are an extension of HMM in which each state is associated with a linear dynamical process. (Fox et al., 2011) describes inference in switching LDS and switching vector autoregressive (VAR) processes.

5.2. Signature

The signature is the estimated mean of the distribution that generated the symbols in the sliding window. In the w -window around time t , the signature is the sample mean x_t of the symbols in the sliding window.

5.3. Evaluation

Given the model $\psi = \langle A, \mu, \Sigma, w \rangle$ and the image O , compute the probability $P(O|\psi)$ that the image was produced by the model. (See Algorithm 5)

Algorithm 5: Evaluation ($O(MNT^d)$)

Input: A, μ, Σ, w_e, O

Output: p

$(X, Q) \leftarrow \text{decoding}(\mu, \Sigma, w_e, O)$ $O(MNT^d)$

$p \leftarrow 1$

for $t \in T^d$ **do** $O(M^2T^d)$
 $p \leftarrow p f(o_t | \mu(q_t), \Sigma(q_t)) \sqrt{\prod_{r \in R(t)} \alpha(X, t) a(q_t, q_r)}$
 $f(o|\mu, \Sigma)$: Normal distribution.
Represent in log domain to prevent underflow.

end

Since the clusters generated by VQ all have the same size, there is no prior probability term in the probability update.

5.4. Decoding

Find the grid configuration $Q = \{q_1, q_2, \dots, q_T\}$, given the model $\psi = \langle A, \mu, \Sigma, w \rangle$ and the image O .

Algorithm 6: Decoding ($O(MNT^d)$)

Input: μ, Σ, w, O

Output: X, Q

Initialize sum

for $t \in T^d$ **do** $O(MNT^d)$
 $x_t \leftarrow \frac{sum}{M}$
 $q_t \leftarrow \text{assign}(\mu, \Sigma, x_t)$ $O(MN)$
increment $sum(\text{newwindow} - \text{oldwindow})$
decrement $sum(\text{oldwindow} - \text{newwindow})$

end

Algorithm 6: We initialize the sliding window and compute the sum of the output instances in it. We slide the sliding window to the end, and in every step, we update the sum and send the signature of the sliding window to *assign* to get the state grid.

5.5. Assign

The *assign* subroutine finds the state $q_t \in S$, given the model $\psi = \langle A, \mu, \Sigma, w \rangle$, and a node signature x_t .

Algorithm 7: Assign ($O(MN)$)

Input: μ, x_t
Output: q_t
for $j \leftarrow 1$ **to** N **do**

 $dist(j) \leftarrow \|x_t - \mu(j)\|$
end
 $q_t \leftarrow \min \text{index}_j(dist_j)$

Algorithm 7: The *assign* subroutine assigns t to that state j for which $\mu(j)$ is the closest to x_t .

5.6. Learning

Optimize the model parameters $\psi = \langle A, \mu, \Sigma, w \rangle$ to best describe how an image comes about, i.e., maximize $P(O|\psi)$. (See Algorithm 8)

Algorithm 8: Learning ($O(MT^d \log T^d)$)

Input: O, w_l
Output: A, μ, Σ

Initialize sum
for $t \in T^d$ **do**

 $x_t \leftarrow \frac{sum}{M}$

 increment $sum(newwindow - oldwindow)$

 decrement $sum(oldwindow - newwindow)$
end
 $(\mu, Q) \leftarrow VQ(X)$

 μ is assigned the VQ codebook.

for $t \in T^d$ **do**

 increment $statecount(q_t)$

 for $r \in R(t)$ **do**

 increment $A'(q_t, r)$

 end

 $y \leftarrow (o_t - \mu(q_t))$

 $\Sigma'(q_t) \leftarrow \Sigma'(q_t) + yy'$
end
for $j \leftarrow 1$ **to** N **do**

 $A(j) \leftarrow \frac{A'(j)}{2d \cdot statecount(j)}$

 $\Sigma(j) \leftarrow \frac{\Sigma'(j)}{statecount(j)}$
end

5.7. Time Complexity

The time complexities are the same as the original model. In case N and M are not considered constant, these caveats apply: (1) In Algorithm 5, $O(M^2T^d)$ is assumed to be less than $O(MNT^d)$, since $O(M)$ is usually less than $O(N)$, and (2) In Algorithm 8, $O(M^2T^d)$ is assumed to be less than $O(MT^d \log T^d)$, since $O(M)$ is usually less than $O(\log T^d)$.

6. Conclusion

In this paper, we have designed a non-markov high-bias low-variance model as an alternative for grid associative CRF. We have two variants: one for grids of discrete symbols, and one for grids of vectors. Our learning algorithm, at time complexity $O(T^d \log T^d)$, is significantly faster than those of general-purpose latent-variable models. We are currently evaluating our model on the PASCAL VOC Challenge 2006 (Everingham et al., 2006), with a focus on learning from small datasets.

6.1. Advantages

1. Variance component of error is low.
2. Uses small datasets efficiently.
3. Computational complexity is low.
4. Easily extends to a quadtree approach.

6.2. Disadvantages

1. Bias component of error is high.
2. Does not use large datasets efficiently.
3. Modeling accuracy is low.
4. N , w , and β are parameters and need to be chosen appropriately.

6.3. Future Work

1. A quadtree approach can provide progressive results.
2. The model can be repeated multiple times, each with a different window size, and combined into a factorial model.
3. A theoretical framework can be developed for guarantees on modeling accuracy.
4. Estimating a belief-state instead of a vanilla state might give better accuracy.
5. N can be learned from the data.
6. w can be learned from the data.

Acknowledgments

C. V. Jawahar, Kamalakar Karlapalem, Balaraman Ravindran, Brendan J. Frey, Gowthaman Arumugam, Harini Ananthapadmanaban, Csaba Szepesvári, P. Prasanna.

References

Baker, James. The Dragon System—An Overview. *IEEE Transactions on Acoustics, Speech and Signal Processing*, 23(1):24–29, 1975.

- Baum, Leonard E. and Petrie, Ted. Statistical Inference for Probabilistic Functions of Finite State Markov Chains. *Annals of Mathematical Statistics*, 37(6):1554–1563, 1966.
- Beal, Matthew J., Ghahramani, Zoubin, and Rasmussen, Carl E. The Infinite Hidden Markov Model. In *NIPS 2001: Proceedings of the Fourteenth Annual Conference on Neural Information Processing Systems*, pp. 577–584, 2002.
- Blake, Andrew, Kohli, Pushmeet, and Rother, Carsten. *Markov Random Fields for Vision and Image Processing*. MIT Press, 2011. ISBN 0262015773, 9780262015776.
- Boykov, Yuri, Veksler, Olga, and Zabih, Ramin. Fast Approximate Energy Minimization via Graph Cuts. *IEEE Transactions on Pattern Analysis and Machine Intelligence*, 23(11):1222–1239, 2001.
- Dietterich, Thomas G. Machine Learning for Sequential Data: A Review. In *Structural, Syntactic, and Statistical Pattern Recognition*, volume 2396 of *LNCIS*, pp. 15–30, 2002.
- Equitz, William H. A New Vector Quantization Clustering Algorithm. *IEEE Transactions on Acoustics, Speech and Signal Processing*, 37(10):1568–1575, 1989.
- Everingham, Mark, Zisserman, Andrew, Williams, Chris K. I., and van Gool, Luc. The PASCAL Visual Object Classes Challenge 2006 Results, 2006.
- Fox, Emily B., Sudderth, Erik B., Jordan, Michael I., and Willsky, Alan S. Bayesian Nonparametric Inference of Switching Dynamic Linear Models. *IEEE Transactions on Signal Processing*, 59(4):1569–1585, 2011.
- Jelinek, Fred. Fast Sequential Decoding Algorithm Using a Stack. *IBM Journal of Research and Development*, 13(6):675–685, 1969.
- Leslie, Christina S., Eskin, Eleazar, and Noble, William Stafford. The Spectrum Kernel: A String Kernel for SVM Protein Classification. In *Pacific Symposium on Biocomputing*, pp. 566–575, 2002.
- Montañez, George D., Amizadeh, Saeed, and Laptev, Nikolay. Inertial Hidden Markov Models: Modeling Change in Multivariate Time Series. In *AAAI 2015: Proceedings of the Twenty-Ninth Conference of the Association for the Advancement of Artificial Intelligence*, 2015.
- Pearl, Judea. *Probabilistic Reasoning in Intelligent Systems: Networks of Plausible Inference*. Morgan Kaufmann Publishers, 1988. ISBN 0-934613-73-7.
- Prince, Simon J. D. *Computer Vision: Models, Learning, and Inference*. Cambridge University Press, 2012. ISBN 1107011795, 9781107011793.
- Rabiner, Lawrence R. A Tutorial on Hidden Markov Models and Selected Applications in Speech Recognition. *Proceedings of the IEEE*, 77(2):257–286, 1989.
- Taskar, Ben, Chatalbashev, Vassil, and Koller, Daphne. Learning Associative Markov Networks. In *ICML 2004: Proceedings of the Twenty-First International Conference on Machine Learning*, 2004.
- Wallach, Hanna M. Efficient Training of Conditional Random Fields. Master’s thesis, University of Edinburgh, 2002.
- Wu, Fa-Yueh. The Potts Model. *Reviews of Modern Physics*, 54(1):235–268, 1982.